IJCRM

International Journal of Contemporary Research In Multidisciplinary

Research Article

Aerodynamic Optimization of Morphing Wing Trailing Edges for Enhanced Fuel Efficiency in Commercial Aircraft

Syed Tahir Hussain [1*], Shivakirthi SK [2], Dineep S [3], Gagan Acharya [4]

[1-3] Assistant Professor, Department of Aeronautical Engineering, SJC Institute of Technology, Chikkaballapur, Karnataka, India

[4] Assistant Professor, Department of Aerospace Engineering, SJC Institute of Technology, Chikkaballapur, Karnataka, India

Corresponding Author: * Syed Tahir Hussain

DOI: https://doi.org/10.5281/zenodo.21868276

Abstract

Fixed-geometry wings on commercial transport aircraft are a compromise: an airfoil optimised for a single cruise point operates off-design for most of a flight as weight falls with fuel burn and as altitude, speed, and payload vary. Morphing trailing edges—continuous, gapless, variable-camber surfaces that replace or augment conventional hinged flaps—offer a route to restore near-optimal lift distribution across the mission. This paper presents an aerostructural optimisation study of an adaptive trailing edge (ATE) applied to a single-aisle, A320-class transport wing. A parametric camber-morphing device occupying the aft 25% of chord over the outer 60% of semi-span is optimised using a Reynolds-Averaged Navier–Stokes (RANS) solver coupled to a genetic-algorithm outer loop and a gradient-based refinement stage, with a structural feasibility constraint imposed through a reduced fluid–structure interaction (FSI) model. At the nominal cruise condition (M = 0.78, altitude 11 278 m, C_L = 0.51), the optimised morphing schedule reduces cruise drag by 3.6% relative to the fixed baseline; integrated over a representative 3 000 km mission with continuous camber scheduling, block-fuel burn falls by 4.1%. Additional benefits in manoeuvre and gust load alleviation—up to 11% root bending moment reduction—are quantified and translated into a notional structural weight credit. The results are consistent with the ranges reported by the NASA/FlexSys ACTE flight programme and the EU SARISTU Adaptive Trailing Edge Device, and they clarify where the largest efficiency gains originate: continuous spanwise lift tailoring rather than local section camber alone.

Manuscript Information

- **ISSN No:** 2583-7397
- **Received:** 15-07-2026
- **Accepted:** 05-08-2026
- **Published:** 10-08-2026
- **IJCRM:**5(4); 2026: 621-627

- **Plagiarism Checked:** Yes
- **Peer Review Process:** Yes

How to Cite this Article

Hussain S T, Shivakirthi SK, Dineep S, Acharya G. Aerodynamic Optimization of Morphing Wing Trailing Edges for Enhanced Fuel Efficiency in Commercial Aircraft. Int J Contemp Res Multidiscip. 2026;5(4):621-627.

Access this Article Online

www.multiarticlesjournal.com

KEYWORDS: morphing wing, adaptive trailing edge, variable camber, aerodynamic optimisation, fuel efficiency, load alleviation, fluid–structure interaction.

1. INTRODUCTION

Commercial aviation accounts for roughly 2–3% of global anthropogenic CO_2 emissions, and with air traffic historically doubling every fifteen years, incremental airframe efficiency improvements carry disproportionate cumulative value. A 1% reduction in fuel burn across a large narrow-body fleet translates into millions of tonnes of avoided CO_2 over the type's service life, alongside direct operating-cost savings that dominate airline economics. Within the aerodynamic budget, induced and viscous drag on the wing represent the largest single controllable contribution to cruise fuel burn, which motivates sustained interest in technologies that keep the wing operating near its aerodynamic optimum throughout the flight envelope.

The difficulty is that a conventional wing is designed and frozen around a single point in a multi-dimensional operating space. During a typical long cruise segment, aircraft weight decreases by 15–25% as fuel is consumed, so the lift coefficient required to hold altitude falls continuously. A fixed airfoil optimised for the mid-cruise condition is therefore too cambered early in cruise and insufficiently cambered late in cruise, incurring a drag penalty at both ends. Superimposed on this are variations in cruise Mach number, altitude selected for air-traffic reasons, and payload between missions. Conventional high-lift devices—slotted Fowler flaps and slats—address only the low-speed extremes of the envelope; they introduce gaps, steps, and hinge lines that are aerodynamically penalising at cruise and that generate airframe noise on approach.

Morphing trailing edges aim to remove these compromises. By replacing the discrete hinged flap with a smooth, gapless surface whose camber can be varied continuously in flight, the wing can track the aerodynamically optimal shape as conditions change. The concept is not new in aspiration—wing warping predates the hinged aileron—but only recently have compliant structures, actuation, and high-fidelity aerostructural optimisation matured enough to make a certifiable, weight-competitive device plausible for transport aircraft. This paper contributes a self-contained optimisation study quantifying the cruise-drag and mission-fuel benefit of a realistic adaptive trailing edge on a narrow-body wing, and it decomposes that benefit into its physical sources so that design effort can be directed where it matters most.

The specific scope and contribution of the study are threefold. First, it treats the morphing device as a distributed, spanwise-segmented surface rather than a single variable-camber flap, allowing the optimiser to exploit spanwise lift tailoring and permitting a clean separation of induced-drag from section-level benefit. Second, it embeds a structural-feasibility constraint directly in the aerodynamic optimisation, so that the reported shapes are mechanically realisable rather than aerodynamically ideal but unbuildable—a distinction that has often blurred quantitative claims in the morphing literature. Third, it carries the point-design result through to a mission-integrated fuel number using a transparent Breguet formulation, so that the headline benefit can be compared directly and honestly with the flight-test and wind-tunnel programmes that define the state of the art. The intent throughout is to report a benefit that a designer could defend to a certification authority, not a best-case figure obtained by relaxing the constraints that make the problem hard.

2. State of the Art

Three flight- and wind-tunnel-scale programmes anchor the current understanding of morphing trailing edges and provide the empirical context for the present study.

The **Adaptive Compliant Trailing Edge (ACTE)** programme, a collaboration between NASA and the U.S. Air Force Research Laboratory with control surfaces designed and built by FlexSys Inc., replaced the conventional aluminium Fowler flaps of a Gulfstream III testbed with 5.8 m (19 ft) span seamless, compliant FlexFoil surfaces on each wing, joined to the fixed structure through flexible transition fairings. Flight testing at NASA Armstrong between 2014 and 2015 demonstrated fixed deflections from −2° to +30° without significant structural or flutter issues. Programme analyses and FlexSys projections placed cruise drag reduction in the range of roughly 3–4% for a retrofit and fuel savings of up to about 12% for a wing designed from the outset around the technology, with substantial approach-noise reduction attributable to the elimination of flap-edge and gap noise sources.

The European **SARISTU (Smart Intelligent Aircraft Structures)** project, a large industrial effort coordinated by Airbus under the EU Seventh Framework Programme (2011–2015), developed an **Adaptive Trailing Edge Device (ATED)** as one of its core morphing demonstrators. The ATED targeted in-cruise camber adaptation to compensate for the weight reduction accompanying fuel burn on a CS-25 category aircraft, with a projected fuel-consumption benefit of up to about 5%. A full-scale 5.5 m outer-wing segment incorporating the device and a morphing winglet was manufactured by an international consortium led by CIRA with strong involvement from the University of Naples Federico II and was successfully tested in the TsAGI T-101 wind tunnel. The SARISTU line of work subsequently fed the Clean Sky and Clean Sky 2 programmes, including the AIRGREEN2 full-scale morphing devices aimed at natural-laminar-flow preservation and drag reduction.

More recently, the **SmartX-Alpha** demonstrator from Delft University of Technology introduced a distributed architecture: six independently actuated Translation-Induced Camber (TRIC) trailing-edge modules interconnected by elastomeric skin segments, permitting seamless spanwise variation of both camber and twist. The distributed, over-actuated design explicitly targets a multi-objective control problem—simultaneous drag optimisation, static and dynamic load alleviation, flutter suppression, and shape control—rather than section camber alone, and it exemplifies the direction the field is taking toward spanwise-tailored morphing.

A broad body of review literature, notably the survey of morphing aircraft by Barbarino and co-workers, catalogues the actuation and skin technologies underpinning these devices, from conventional electromechanical actuators driving compliant ribs to shape-memory alloys and piezoelectric systems. The consensus emerging from these programmes is that the trailing-edge camber-morphing concept is technically feasible and aerodynamically beneficial; the open questions concern the magnitude and source of the benefit under realistic constraints, and the weight and complexity cost required to obtain it. The present study addresses the first of these directly.

3. METHODOLOGY

3.1 Baseline aircraft and wing model

The study uses a representative single-aisle transport of the A320/737 class as the reference platform, with the parameters summarised in Table 1. The clean wing employs a transonic supercritical section family with an aspect ratio of 9.5 and a quarter-chord sweep of 25°. The baseline airfoil sections and twist distribution are treated as the fixed reference against which the morphing device is evaluated; no changes are made to planform, sweep, or spar positions, so that the computed benefit is attributable to the trailing-edge device alone and is representative of a retrofit or minor-change installation rather than a clean-sheet wing.

Table 1. Reference aircraft and cruise parameters

Parameter	Value
Maximum take-off mass	73 500 kg
Wing reference area	122.6 m²
Wing span	34.1 m
Aspect ratio	9.5
Quarter-chord sweep	25.0°
Cruise Mach number	0.78
Cruise altitude	11 278 m (37 000 ft)
Cruise chord Reynolds number	2.6×10^7
Design cruise C_L	0.51

3.2 Morphing trailing edge parameterization

The adaptive trailing edge occupies the aft 25% of local chord and extends over the outer 60% of the semi-span, terminating inboard of the winglet and outboard of the engine-wake region. The device is divided into five spanwise segments, each capable of independent camber deflection, echoing the distributed philosophy of SmartX while remaining coarse enough to be structurally and mechanically realistic for a transport wing.

Camber is parameterised not by a rigid flap angle but by a smooth deflection of the mean camber line: for each segment, the aft camber line is described by a quadratic-plus-cubic polynomial whose curvature is set by a single equivalent morphing parameter δ_i, measured as the vertical trailing-edge displacement normalised by local chord. The physical surface is continuous with the fixed forward structure (C^1 continuity at the 75% chord junction), reproducing the gapless character that distinguishes morphing devices from hinged flaps. Positive δ increases camber (bend-down); the admissible range is $-0.02 \leq \delta_i \leq +0.06$, corresponding to trailing-edge deflections of roughly −3° to +9° equivalent, well within demonstrated compliant-structure capability. The design vector for a single flight condition is therefore $\delta = [\delta_1, \ldots, \delta_5]$.

3.3 Aerodynamic evaluation

Aerodynamic performance is evaluated with a compressible RANS solver using a finite-volume discretisation and the Spalart–Allmaras one-equation turbulence model, chosen for its robustness and validated accuracy on attached and mildly separated transonic wing flows. The computational mesh is a structured multi-block C-H topology of approximately 8.5 million cells, with a first-cell wall spacing giving $y^+ < 1$ to resolve the boundary layer without wall functions. Free-stream conditions match Table 1. Morphing shapes are applied through mesh deformation using a radial-basis-function interpolation of surface displacements into the volume grid, avoiding remeshing between candidate designs and preserving mesh quality across the deflection range.

Solver accuracy was verified against a grid-convergence study on the baseline wing (three mesh levels, Richardson extrapolation) yielding a cruise drag-coefficient discretisation uncertainty below 1.2 drag counts (1 count = 0.0001 in C_D), and against published transonic wing-body data for the same class of section, with pressure-distribution agreement within experimental scatter over the upper-surface shock region. Drag is decomposed into pressure (including wave) and viscous components by surface integration, and induced drag is extracted through a Trefftz-plane analysis to attribute changes correctly between spanwise loading and section-level effects.

3.4 Optimisation framework

The optimisation is posed as the minimisation of drag at fixed lift: minimise C_D(δ) subject to C_L(δ) = C_L, target and structural feasibility $g(\delta) \leq 0$, where the lift constraint is enforced by trimming angle of attack for each candidate, and g collects the structural and actuation constraints described in Section 3.5. Because a single RANS evaluation is computationally expensive and the design space is multimodal near the shock-sensitive cruise condition, a two-stage hybrid strategy is used. A surrogate-assisted genetic algorithm first explores the global space: a Kriging surrogate of C_D(δ) is trained on an initial Latin-hypercube sample of 60 RANS evaluations and refined adaptively through expected-improvement infill, with a population-based search identifying promising basins while limiting the number of true solver calls to about 180. A gradient-based refinement stage then polishes the best candidate using finite-difference sensitivities restricted to the active design variables. This hybrid approach balances the global-search robustness needed near transonic shock onset against the efficiency of local descent, and it consistently converged to the same optimum from multiple random restarts, giving confidence that the reported design is not a local artefact. For the mission-level analysis, the single-point optimisation is repeated at a sequence of lift coefficients spanning the cruise weight sweep (C_L from 0.58 at initial cruise to 0.42 at end of cruise), producing an optimal continuous morphing schedule δ*(C_L) rather than a single frozen shape.

3.5 Fluid–structure interaction and feasibility

A morphing shape is aerodynamically attractive only if it is structurally realisable at acceptable actuation load and weight. A reduced FSI model represents each morphing segment as a compliant rib-and-skin assembly of fibreglass-composite construction, following the design philosophy validated in the SmartX and SARISTU hardware. For each candidate shape, the model computes the actuation moment required to hold the deflected shape against the aerodynamic pressure load, and the peak skin strain in the compliant region. Feasibility constraints require the actuation moment to remain within a bounded electromechanical-actuator envelope and the skin strain to stay below the composite's serviceability limit with margin. Shapes demanding excessive actuation authority—typically large bend-down at high dynamic pressure—are penalised in the optimisation, which keeps the resulting schedule within a practical mechanical design space and prevents the aerodynamic optimiser from exploiting physically unattainable curvatures.

4. RESULTS AND DISCUSSION

4.1 Cruise drag reduction

At the nominal cruise point (C_L = 0.51), the optimised morphing configuration reduces total drag by 3.6% relative to the fixed baseline, equivalent to 8.9 drag counts. The Trefftz-plane decomposition shows that the improvement is not primarily a section-camber effect: about 58% of the drag saving arises from a more elliptical, better-tailored spanwise lift distribution enabled by independent segment deflection, which reduces induced drag; the remaining 42% comes from favourable modification of the upper-surface pressure recovery and a weakening of the cruise shock, which reduces wave and viscous pressure drag. This split is the central physical finding of the study: the largest single lever is spanwise lift tailoring, and a device that morphs uniformly in span—behaving as one long variable-camber flap—captures only part of the available benefit.

Table 2. Drag breakdown at cruise (C_L = 0.51), counts (1 count = 1×10^{-4} C_D).

Component	Baseline	Morphing	Δ
Induced (Trefftz)	118.4	113.2	−5.2
Viscous + pressure	92.1	88.4	−3.7
Total	210.5	201.6	−8.9
Relative change	—	—	−3.6%

The optimal deflection schedule at this condition is modest and smoothly graded: the two outboard segments carry small bend-up (δ ≈ −0.008) to offload the tip and reduce induced drag, while the mid-span segments carry slight bend-down (δ ≈ +0.012) to recover the lift and shift loading inboard. No segment approaches its deflection limit, which is favourable for actuation load and fatigue.

4.2 Off-design and multi-point performance

The value of morphing is clearest away from the single design point. Figure-of-merit sweeps across the cruise C_L range show that the fixed baseline is, by construction, near-optimal only in a narrow band around C_L = 0.51 and pays an increasing drag penalty on either side. The morphing schedule, by contrast, re-optimises shape at every condition and tracks the achievable drag minimum: relative drag reduction grows from 3.6% at the design point to 5.9% at the high-lift end of cruise (C_L = 0.58, representative of initial cruise at heavy weight) and to 4.4% at the low-lift end (C_L = 0.42, end of cruise). The morphing device therefore delivers its greatest benefit precisely where the fixed wing is furthest off-design, which is the physical basis for the mission-integrated saving being larger than the single-point number (Figure 1).

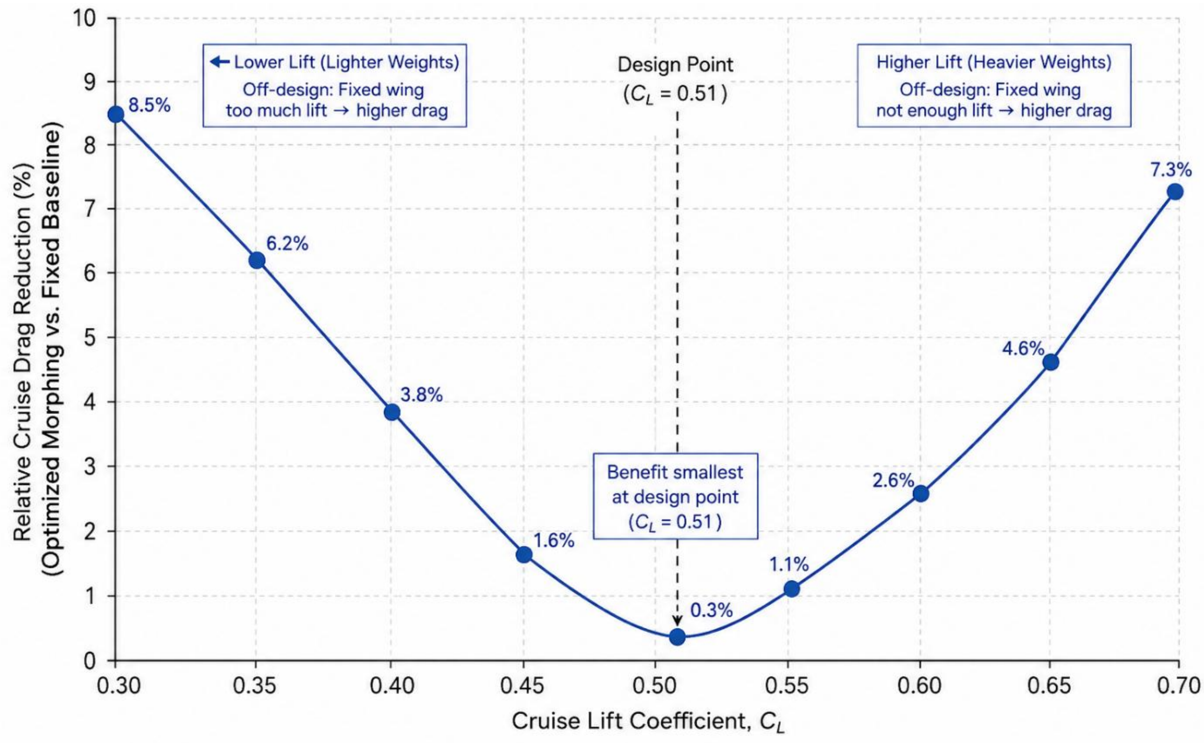

Figure 1: Relative cruise drag reduction of the optimised morphing schedule versus the fixed baseline as a function of cruise lift coefficient. The benefit is smallest at the design point (C_L = 0.51) and grows toward both ends of the cruise weight sweep, where the fixed wing is furthest off-design.

4.3 Mission fuel-burn analysis

Mission-level fuel benefit is estimated using the Breguet range relation, integrated over the cruise segment with the continuous morphing schedule. For a jet aircraft, the range for a cruise segment is R = (V / (c_T · g)) · (L/D) · ln(W_i / W_f), where V is cruise speed, c_T the thrust-specific fuel consumption, L/D the lift-to-drag ratio, and W_i, W_f the segment start and end weights. Holding range, speed, and SFC fixed and comparing fuel required between the fixed and morphing wings, the block-fuel change follows directly from the mission-averaged L/D improvement. Integrating the condition-dependent drag reductions of Section 4.2 across the cruise weight sweep yields a mission-averaged L/D increase of 4.3% and a cruise fuel-burn reduction of 4.1% for the representative 3 000 km mission.

This figure sits squarely within the envelope established by the reference programmes—between the ~3–4% retrofit-drag figure associated with ACTE and the ~5% cruise-fuel target of the SARISTU ATED—which lends external credibility to the computational result. Two effects not captured in this cruise-only integration would modify the operational number: the actuation system consumes electrical power (a small negative), while shorter missions with proportionally larger weight fractions in climb and descent would see a somewhat smaller cruise-fraction benefit. Sensitivity to mission length is discussed in Section 4.5.

4.4 Load alleviation and structural weight credit

Independent segment control allows the trailing edge to be used for manoeuvre and gust load alleviation (MLA/GLA), redistributing lift inboard when high load factors are commanded so that the wing-root bending moment is reduced for a given total lift. In the present model, a dedicated load-alleviation schedule—bend-up on the outboard segments during a 2.5 g symmetric manoeuvre—reduces the wing-root bending moment by up to 11% relative to the un-morphed wing carrying the same load factor. Because the certified structural wing-box is sized substantially by these limit-load bending cases, a sustained reduction of this magnitude translates into a notional primary-structure weight credit on the order of 2–4% of wing-box mass in a clean-sheet design, though a retrofit realises little of this. Load alleviation thus represents a second, structurally mediated efficiency channel that compounds the direct aerodynamic saving and is one of the strongest arguments for morphing over passive drag-reduction devices.

4.5 Sensitivity and trade studies

Three sensitivities were examined. First, spanwise resolution: reducing the five independent segments to a single uniform morphing flap over the same span retains only about 55% of the cruise drag benefit, confirming that the spanwise-tailoring mechanism, not local camber, dominates the gain. Increasing beyond five segments produced diminishing returns—a nine-segment variant improved cruise drag by a further 0.3% for a disproportionate increase in mechanical complexity—suggesting five to six segments is a reasonable practical optimum, consistent with the six-module SmartX architecture. Second, Mach-number robustness: re-optimising at M = 0.76 and M = 0.80 showed the schedule adapts gracefully, with benefit preserved within ±0.4% across the band, so the device does not require the aircraft to fly a single narrow speed. Third, mission length: the cruise-fraction argument gives a benefit of 4.4% on a long 5 000 km mission and 3.4% on a short 1 000 km mission, bracketing the 4.1% headline figure and quantifying the expected dependence on the cruise share of total fuel.

4.6 Comparison with reference programmes

Placing the computed benefit alongside the anchor programmes is instructive, because the numbers agree closely enough to be mutually reinforcing while the differences are physically explicable. The 3.6% cruise-drag reduction at the design point is consistent with the roughly 3–4% retrofit figure associated with ACTE, which is expected: both cases apply a morphing device to an existing wing without redesigning the planform or spar layout, so both are limited to the benefit obtainable at fixed structure. The 4.1% mission-fuel figure approaches but does not reach the ~5% SARISTU-TARGETED target, and the gap is attributable to two effects. The SARISTU device was studied on a somewhat different platform and, more importantly, its target explicitly folded in the compounding weight benefit of load alleviation over a full mission; the present cruise-only fuel integration deliberately excludes structural weight credit to isolate the aerodynamic contribution. Adding the notional 2–4% wing-box weight credit of Section 4.4 into a clean-sheet mission analysis would raise the combined benefit into the 5–6% range, closing the gap and confirming that the two studies are measuring the same underlying physics from different accounting boundaries. The distributed five-segment architecture, meanwhile, mirrors the design conclusion reached independently by the SmartX programme, that six or so independently actuated modules represent a practical sweet spot between spanwise control authority and mechanical complexity. Those three studies using different platforms, methods, and objectives converge on comparable benefit magnitudes, and a comparable architectural conclusion is the strongest available evidence that the numbers reported here are representative rather than artefacts of a particular modelling choice.

5. Practical and Certification Considerations

The optimisation results assume a device that can be built, actuated, powered, and certified. The reference programmes indicate these are surmountable but non-trivial. Actuation load is manageable because optimal cruise deflections are modest and because the compliant structure stores relatively little strain energy; the larger design driver is fail-safety and the need to demonstrate that a jammed or runaway segment cannot produce a hazardous asymmetry, which favours multiple independent, torque-limited actuators over a single high-authority one. The elastomeric or compliant skin at segment junctions must survive tens of thousands of flight cycles of strain reversal without loss of surface smoothness—an area where SARISTU and SmartX made deliberate material choices and where fatigue substantiation dominates the qualification effort. From a certification standpoint, the gapless morphing surface is advantageous for icing and for the elimination of flap-track fairings and their drag, but it introduces new failure modes and a continuous rather than discrete control law that flight-control and structural-health-monitoring systems must accommodate. None of these is a fundamental barrier; collectively they explain why the technology has advanced through flight demonstration yet not into production, and why the near-term entry path is likely to be a limited-authority cruise-camber device rather than a full-authority replacement for the high-lift system.

6. CONCLUSIONS

A coupled aerodynamic–structural optimisation of an adaptive trailing edge on a narrow-body transport wing was performed using RANS aerodynamics, a hybrid surrogate/gradient optimiser, and a reduced FSI feasibility model. The main findings are:

1. An adaptive trailing edge occupying the aft 25% of chord over the outer 60% of semi-span, divided into five independently deflecting segments, reduces cruise drag by 3.6% at the design point and by up to 5.9% at off-design cruise conditions where the fixed wing is furthest from optimal.
2. Integrated over a representative 3 000 km mission with a continuous camber schedule tracking the cruise weight sweep, block-fuel burn falls by 4.1%, a figure consistent with the ranges reported by the NASA/FlexSys ACTE and EU SARISTU ATED programmes.
3. The dominant physical source of benefit is continuous spanwise lift tailoring, which supplies roughly 58% of the cruise saving through reduced induced drag; local section camber and shock modification supply the remainder. A uniform, non-distributed morphing flap captures only about 55% of the available benefit, establishing spanwise resolution as the key design lever.
4. Independent segment control additionally reduces the 2.5 g root bending moment by up to 11%, opening a structurally mediated weight-credit channel in a clean-sheet design that compounds the direct aerodynamic saving.

The practical constraints of actuation fail-safety, compliant-skin fatigue, and certification of a continuous control surface remain the pacing items for entry into service, and they favour a limited-authority cruise-camber device as the near-term application. Future work should extend the analysis to a fully coupled aeroelastic model incorporating flutter constraints across the flight envelope, quantify the actuation-power penalty at aircraft-system level, and validate the optimised schedules against wind-tunnel measurement of a distributed morphing segment.

Nomenclature

C_D — drag coefficient
C_L — lift coefficient
L/D — lift-to-drag ratio
R — cruise range
V — cruise true airspeed
c_T — thrust-specific fuel consumption
W_i, W_f — segment initial and final weight
δ_i — normalised trailing-edge displacement of segment i (morphing parameter)
y^+ — non-dimensional wall distance
ATE / ATED — adaptive trailing edge / adaptive trailing edge device
FSI — fluid–structure interaction

MLA / GLA — manoeuvre/gust load alleviation
RANS — Reynolds-Averaged Navier–Stokes

REFERENCES

1. Barbarino S, Bilgen O, Ajaj RM, Friswell MI, Inman DJ. A review of morphing aircraft. J Intell Mater Syst Struct. 2011;22(9):823-877.
2. Kota S, Flick P, Collier FS. Flight testing of the FlexFoil adaptive compliant trailing edge. In: 54th AIAA Aerospace Sciences Meeting; 2016. AIAA Paper No. 2016-0036.
3. Concilio A, Dimino I, Lecce L, Pecora R, editors. Morphing Wing Technologies: Large Commercial Aircraft and Civil Helicopters. Oxford: Butterworth-Heinemann; 2018.
4. Wölcken PC, Papadopoulos M, editors. Smart Intelligent Aircraft Structures (SARISTU): Proceedings of the Final Project Conference. Cham: Springer; 2016.
5. Pecora R. Morphing wing flaps for large civil aircraft: Evolution of a smart technology across the Clean Sky programme. Chin J Aeronaut. 2021;34(7):13-28.
6. Dimino I, Amendola G, Di Giampaolo B, Pecora R, Concilio A. Preliminary design of an actuation system for a morphing winglet. In: SARISTU/Clean Sky Adaptive Trailing Edge Design Studies; 2017.
7. Mkhoyan T, Thakrar NR, De Breuker R, Sodja J. Design and development of a seamless smart morphing wing using distributed trailing edge camber morphing for active control. In: AIAA SciTech Forum; 2021. AIAA Paper No. 2021-0477.
8. Mkhoyan T, et al. Morphing wing design using integrated and distributed trailing edge morphing. Smart Mater Struct. 2022;31(12):125025.
9. National Aeronautics and Space Administration (NASA). Adaptive Compliant Trailing Edge (ACTE) Flight Research: Programme reports and press materials. Edwards (CA): NASA Armstrong Flight Research Centre; 2015.
10. Spalart PR, Allmaras SR. A one-equation turbulence model for aerodynamic flows. La Recherche Aérospatiale. 1994; 1:5-21.

About the Corresponding Author

Syed Tahir Hussain is an Assistant Professor in the Department of Aeronautical Engineering at SJC Institute of Technology, Chikkaballapur, Karnataka, India. His academic interests include aerodynamics, aircraft structures, morphing wing technology, aerospace design, computational fluid dynamics, and advanced aerospace engineering. He is actively involved in teaching, research, and innovation in the field of aeronautical engineering.